Journal of Microelectronics and Electronic Packaging (2012) **9**, 65-77
Copyright © International Microelectronics And Packaging Society
ISSN: 1551-4897

Comparison of Gold and Copper Wire Bonding on Aluminum and Nickel-Palladium-Gold Bond Pads for Automotive Application

Tu Anh Tran,[1] Varughese Mathew,[1] and Harold Downey[2]

Downloaded from http://meridian.allenpress.com/jmep/article-pdf/9/2/65/2248335/imaps_325.pdf by guest on 01 November 2022

***Abstract*—New automotive specifications derived from higher module integration and more stringent environmental requirements expect plastic packages to operate at higher junction temperatures with prolonged duration. Temperature is a key accelerating factor for failures in electronic package devices because of the thermo-mechanical, metallurgical and chemical properties of the materials used in the package. Failures in conventional plastic package at high temperatures such as 175 °C often originate from aluminum – gold wirebonding system because of the formation of Au-Al intermetallic phases and associated Kirkendall voiding which degrades the interface. Methods to overcome such reliability issues in wire bonded devices are to change either the wire material or the bond pad metallurgy or pad finishing other than aluminum which can reliably withstand operations at higher temperature and longer duration.**

***Keywords*—Au wire, Cu wire, electroless Ni/Pd/Au, automotive reliability**

Introduction

New automotive requirements expect plastic packages to survive higher operating temperatures with extended thermal duration. Mission profiles for under-the-hood and transmission application historically specified minimal duration at maximum junction temperature, such as 50 h total at 150°C, while keeping most of the total operating duration at lower temperatures. Further module integration and more stringent environmental requirements push modules and thus plastic packages closer to the heat source. As such, new mission profiles include more than 3500 h total at 150°C. To satisfy new automotive requirements, plastic packages must meet AEC Grade 0 or higher. One key limitation of the conventional plastic package is the use of gold bond wire on aluminum bond pad. Au-Al intermetallic degradation due to intermetallic transformation in high temperature storage condition remains the main reliability concern.

More reliable intermetallic systems have been proposed that change the wire material and/or the bond pad metallization. The use of copper wire bonding is growing very rapidly due to the high cost of gold wire. Copper wire has many benefits, including low cost, high electrical and thermal conductivities, and excellent reliability with aluminum pad metallization. Markets that have seen the largest growth in Cu wire bonded products have been consumer, portable, and industrial electronics. Cu wire has seen limited use in the high reliability automotive markets in some products that used large diameter Cu wire (e.g., 50 μm), but the lower cost benefit of Cu wire makes it desirable for a broader range of automotive products. Since it is well known that the Cu-Al intermetallic compounds (IMCs) form and grow much more slowly than Au-Al intermetallics, the possibility of Cu wire bonding on Al pads meeting reliability requirements is being investigated [1].

Over pad metallization (OPM) is a method whereby pad remetallization using nickel/palladium, nickel/gold, or nickel/palladium/gold over an aluminum bond pad or a copper bond pad offers a noble and reliable metal interconnect. Au wire bonding on OPM is a major area of investigation, but it is burdened with the cost of the Au wire and the OPM processing. Cu wire bonding on OPM is also of interest to reduce the cost of Au wire on OPM, in the event that Cu wire on Al pads is unable to meet all reliability requirements for the most severe environments.

The greater hardness of Cu wire demands careful material selection and bond process optimization. The greater hardness of Cu wire can cause lateral displacement of Al pad metal (e.g., Al splash) during bonding that can cause damage. The lower stress required to form ball bonds with softer Cu wires, and softer Cu free air balls, results in lower Al splash and less risk of damage [2]. Device bond pads on newer semiconductor technology nodes, using low K-Cu structures, are susceptible to damage during bonding, even with Au wire. The risk of pad damage during bonding, and long term reliability degradation, increases with decreasing bond pad pitch due to the use of smaller diameter wires, and the formation of smaller diameter ball bonds. The OPM provides the additional benefits of reducing risk of bonding damage (i.e., armoring the pad) and the elimination of intermetallics as the bond phase between the wire and the OPM, allowing the use of lower stress Cu wire bond parameters, and elimination of pad metal splash.

A. Experimental Planning

The 300 mm test vehicle used in this study was fabricated in 90 nm CMOS copper technology with six metal layers and a 1.2 μm Al cap layer with 0.5% Cu [3]. The die size is 7.2 × 6.3 × 0.28 mm. The baseline Al pad structure used on this test vehicle

Manuscript received February 2012 and accepted June 2012
[1]Freescale Semiconductor Inc., 6501 William Cannon Drive West, Mail Drop: TX30-OE21: Austin, Texas 78735
[2]Retired.
*Corresponding author; email: Tu.Anh.Tran@freescale.com

doi:10.4071/imaps.325
1551-4897 © 2012 International Microelectronics And Packaging Society

is illustrated in Fig. 1. Bond pads were designed using aggressive bond over active (BOA) rules having signal, power, and ground rails running directly underneath the bonding region. The bond pad passivation opening is 52 μm and the minimum pitch is 64 μm. Some wafers were processed with the standard Al cap and others were processed further with OPM. Alternative OPM stack-ups can be nickel/palladium, nickel/gold, or nickel/palladium/gold remetallization over the aluminum bond pad. A cost-competitive electroless Ni/electroless Pd/immersion Au plating process is available for the 300 mm wafer format. This study focused only on the electroless Ni/Pd/Au process. Fig. 2 provides the cross section of Ni/Pd/Au remetallization over the baseline Al pad.

A Ni/Pd/Au bond pad finish is required to achieve high temperature stability and also to provide a stronger bond pad than Al which protects the underlying dielectric layers from possible damage due to bonding force and resulting cratering. Even though thicker OPM is beneficial for minimizing and eliminating cratering, a thinner OPM is preferred from the point of view of a possible electrical short. As the electroless plating is achieved by isotropic growth, it mushrooms as it grows beyond the passivation height. Depending on the pad separation, the OPM height needs to be limited to avoid bridging and a subsequent electrical short. In addition, as the OPM height increases, there is a possibility of stress-related structural defects such as passivation cracking. Because of all these factors, it is important to optimize the OPM height. The minimum spacing between unrelated passivation openings is 12 μm on the test vehicle. With the passivation thickness of about 1 μm, three Ni thicknesses were evaluated, 1 μm, 2 μm, and 3 μm. Pd and Au thickness were held constant at 0.3 μm and 0.05 μm, respectively. Process defects on as-plated Ni/Pd/Au bond pads such as color difference and surface roughness affecting yield will be discussed in the next section.

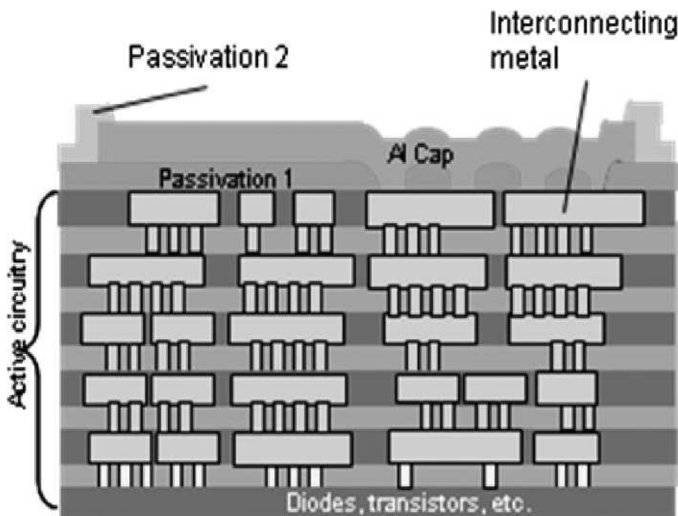

Fig. 1. Test vehicle bond pad with bond-over-active structure, with baseline Al cap.

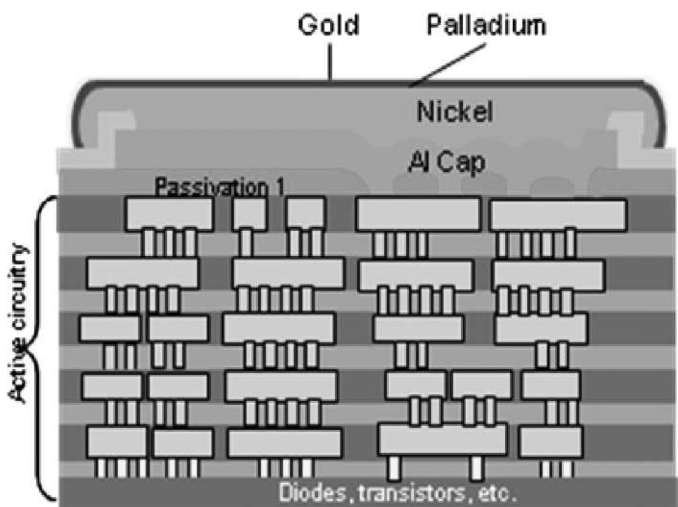

Fig. 2. Test vehicle bond pad with bond-over-active structure, with Ni/Pd/Au remetallization.

Wafers with baseline Al bond pads and with Ni/Pd/Au remetallization were provided for this evaluation. The test dice were assembled into a 176 lead 24 × 24 mm 0.5 mm pitch LQFP package using standard assembly processes. Wire bonding was done with 23 μm 2 N Au wire and 4 N Cu wires on both Al bond pad and Ni/Pd/Au bond pad. The 2 N Au wire was selected for highest reliability performance of Au-Al intermetallics in extended thermal duration. Au wire bond process parameters were first optimized on the Al bond pad, and then verified and adjusted on OPM bond pads. Similarly, Cu wire bond process parameters were first set up for an Al pad. Cu wire bonding on an Al pad required more careful optimization to ensure reliable bonding with minimal Al splashing and appropriate Al remnant underneath the ball bond. Once the wire bond parameters were established for the Al pad, the recipe was tried out on the Ni/Pd/Au pad. Minimal adjustment was needed for the Ni/Pd/Au pad. The ball bond diameter was targeted to be 43 μm nominal.

Wire bonded strips without mold encapsulation were thermally aged at 225°C in a nitrogen purged oven for 96, 192, 504, and 1008 h. Very high baking temperature and long duration were selected in order to bring out differentiating performance between wire material types and pad types in applications with high temperature and extended duration. At each internal, strips were removed and submitted to ball shear and wire pull data collection for ball bond interconnect integrity assessment. Completed assembled packages were submitted to standard package reliability testing. Package-level reliability testing began with moisture sensitivity level 3 (MSL3) preconditioning (10 cycles of temperature cycling at −65°C to 150°C, bake at 125°C/24 h, moisture soak at 30°C, 60%RH for 192 h, and three cycles of forced convection reflow at 260°C). After MSL3 preconditioning, parts were split and subjected to air-to-air temperature cycling (−65°C to 150°C) for 500, 1000, 1500, 2000, 2500, and 3000 cycles, and unbiased HAST (highly accelerated stress test, UHAST; 130°C/85%RH/33.3 PSIA) for 96, 192, and 240 h. Other packages were submitted directly to high temperature bake at 175°C without MSL preconditioning for 540, 1080, 1620, and 2160 h. An electrical test was performed after all stress readpoints. Some packages were retained at various stress readpoints, deprocessed, and submitted to ball shear and wire pull tests. AEC grade 0 requires passing an electrical test after 2000 cycles of temperature cycling, 96 h of UHAST, and 1000 h of high temperature bake at 175°C. Cross-sectioning through the

Downloaded from http://meridian.allenpress.com/jmep/article-pdf/9/2/65/2248335/imaps_325.pdf by guest on 01 November 2022

ball bonds was also conducted to examine the welding region between the ball bond and bond pad.

B. OPM Process Defect and Yield Impact

As the OPM (or Ni/Pd/Au stack) process is an end-of-line (EOL) step, it is very important to understand the impact of plating defects on the process yield. Extensive examination was carried out to identify various plating defects to determine the ones affecting yield. Color variations within the plated bonding pads were observed upon optical inspection as shown in Fig. 3a. The appearance shown in Fig. 3b was identified as relatively low roughness through SEM imaging. No related yield issues were observed with this level of roughness.

However, there were pronounced color variations, which sometimes appeared as black spots on optical inspections, and were found to be yield-affecting defects. Predominantly two types of such defects were observed. The first type of color variations is shown in Figs. 4a and 4b and was found to be due to very nonuniform plating of nickel within an Al bond pad. In Fig. 5, a focused ion beam (FIB) cross section through the bond pad showed that nickel was plated very nonuniformly but the Pd and Au plating was found to be plated as expected.

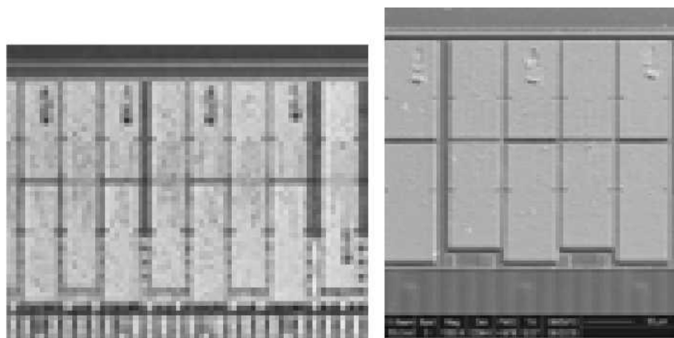

(a) Optical Picture **(b) SEM Picture**

Fig. 3. Minor OPM plating roughness, no yield impact.

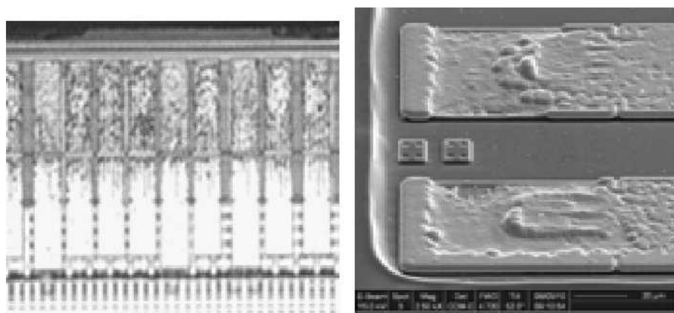

(a) Optical Picture **(b) SEM Picture**

Fig. 4. Rough OPM plating, NSOP impact.

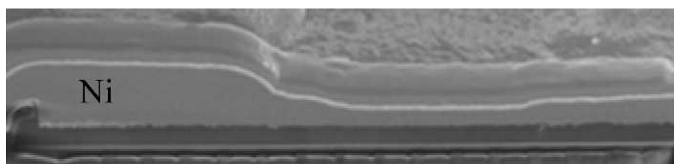

Fig. 5. FIB cross section of rough OPM plating due to nonuniform Ni plating.

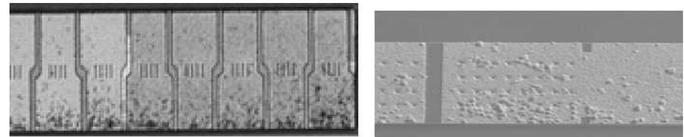

(a) Optical Picture **(b) SEM Picture**

Fig. 6. Black spots on OPM plating, NSOP impact.

Wire bonding on such pads resulted in nonstick-on-pad (NSOP) yield problems.

The second type of color variations which usually appeared as black spots optically is shown in Fig. 6a. SEM imaging in Fig. 6b and FIB cross section in Fig. 7 showed that this defect was due to extraneous growth of Au, leading to an Au thickness of about 5-7 times the expected thickness (instead of 0.03 μm to 0.05 μm) with a thorny appearance.

Energy-dispersive x-ray spectroscopy (EDX) analysis in Fig. 8 showed the presence of Ni in the Pd layer. It was observed that with a nondefective plating of Ni/Pd/Au stack, even a Pd layer of 0.2 μm thickness is a very effective diffusion barrier for Ni and therefore Ni should not be detected in the Pd layer. Hence it appears that the Pd film formed on pads shown in Fig. 6 is defective enough to allow diffusion of Ni which accelerates Au plating to an unexpected thickness and appearance. This inference is supported by the fact the immersion Au plating is not expected to grow Au to a thickness of 0.3 μm, as it is a substitution process.

Wire bonding on OPM pads with thorny Au led to NSOP as shown in Fig. 9a. An FIB cross section of the NSOP pad in Fig. 9b confirmed the thorny growth of Au as mentioned above.

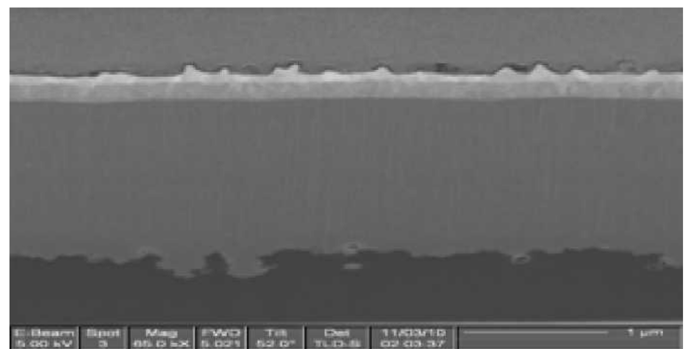

Fig. 7. FIB cross section of rough OPM plating due to extraneous Au plating.

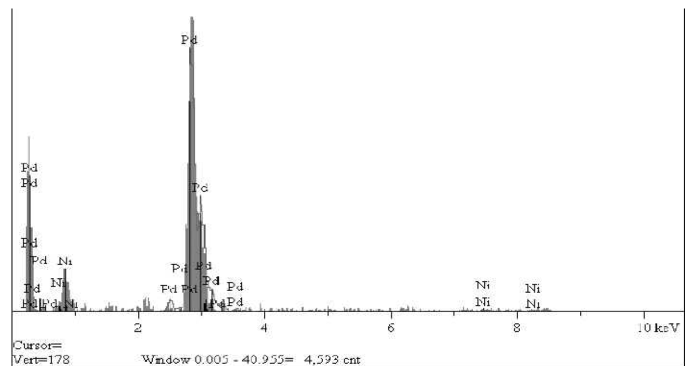

Fig. 8. EDX spectrum of Pd layer from a rough thorny OPM pad.

Downloaded from http://meridian.allenpress.com/jmep/article-pdf/9/2/65/2248335/imaps_325.pdf by guest on 01 November 2022

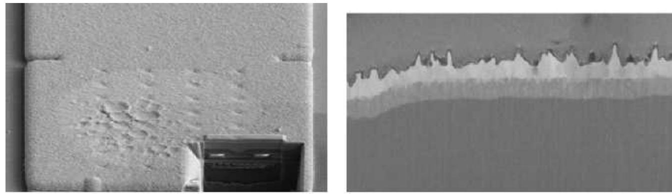

(a) SEM Picture of NSOP **(b) FIB Cross-section**

Fig. 9. NSOP due to rough and thorny Au plating.

Another rare but very optically visible defect observed is shown in Fig. 10 whereby a portion of the OPM was peeled off the Al pad. This defect is due to the poor adhesion of Ni to Al and is generally associated with the presence of bond pad contamination such as carbon and oxides of silicon prior to plating.

All of the aforementioned plating defects cannot be detected by electrical tests of the OPM pads. Hence, an inspection system needs to be established in order to detect these defects. Other defects observed which can cause yield loss were nodular growth along the edges of the pads causing bridging and shorting, as shown in Fig. 11. The probability of electrical shorts due to such nodular growth depends on the separation of bond pads and the height of the passivation surrounding the Al pads. This type of plating defect is detected by post-OPM probing and electrical testing at the final test.

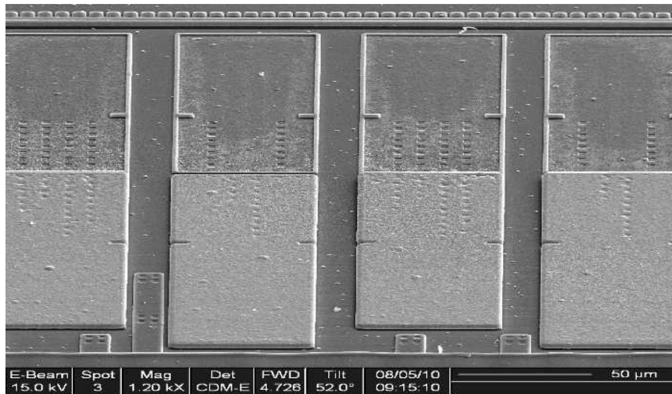

Fig. 10. SEM picture of OPM peeling from Al pad due to poor adhesion.

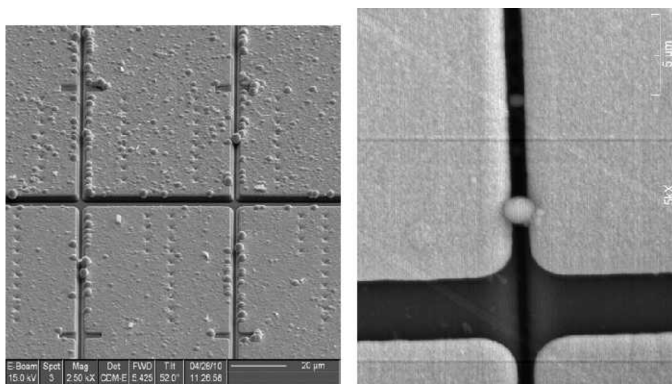

(a) Nodule Growths **(b) Higher Magnification**

Fig. 11. SEM picture of nodular growth leading to electrical short.

C. Strip Level Thermal Aging Results

Fig. 12 shows ion mill cross section micrographs of the Au ball on a baseline Al pad and a 1.3 µm Ni/Pd/Au pad with minimal thermal treatment (i.e., 5 h at 175°C). As expected, Au-Al intermetallics were present in the baseline system. No evidence of intermetallics was found with Au wire on Ni/Pd/Au pad.

Fig. 13 provides ion mill cross-section micrographs of Cu ball on Al pad and 1.3 µm Ni/Pd/Au pad with no thermal aging. Al splashing commonly seen with Cu wire bonding on Al pad as shown in Fig. 13a was completely eliminated when Cu wire bonding on Ni/Pd/Au pad in Fig. 13b. With nickel being about four times as hard as aluminum, there was no metal splashing, and no metal thinning under the ball bond. A slight Al deformation under 1.3 µm Ni/Pd/Au remetallization

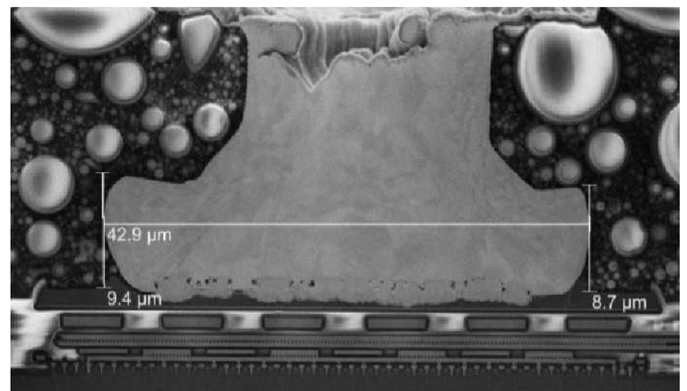

(a) Au Ball on Al Pad – Baseline

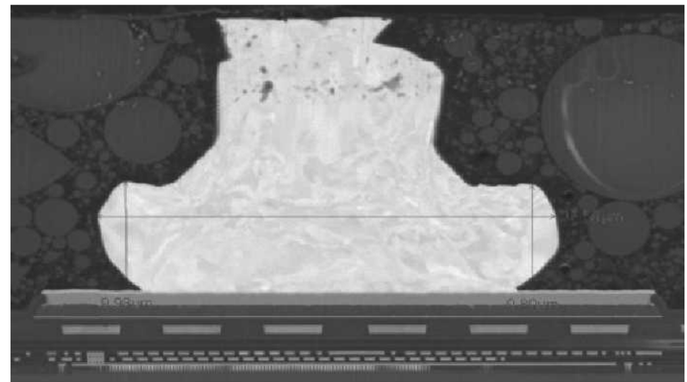

(b) Au Ball on 1.3µm Ni/Pd/Au Pad

Fig. 12. As bonded Au ball on Al pad and OPM pad.

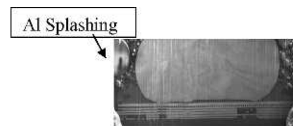

(a) Cu Ball on Al Pad – With Al Splashing

(b) Cu Ball on 1.3µm Ni/Pd/Au Pad – No Al Splashing but Slight Al Deformation

Fig. 13. As bonded Cu ball on Al pad and OPM pad.

Downloaded from http://meridian.allenpress.com/jmep/article-pdf/9/2/65/2248335/imaps_325.pdf by guest on 01 November 2022

Table I
Ball Shear Strength (gf) After 225°C Strip-Level Thermal Aging

		0	96	192	504	1008	1512	2016
Au Wire/Al Pad	Min	13.687	22.51	23.69	12.47	11.35		
	Avg	15.064	25.57	26.77	14.99	15.83		
	Max	15.83	28.69	31.48	18.47	23.39		
	Stdev	0.50	1.66	1.88	1.63	3.25		
	Ball shear %	100%	100%	100%	100%	100%		
	Ball lift	0%	0%	0%	0%	0%		
Au Wire/Ni/Pd/Au Pad	Min	19.94	20.08	20.33	20.37	21.39		
	Avg	22.63	21.24	21.47	21.38	22.65		
	Max	25.20	24.05	22.95	22.41	24.03		
	Stdev	1.53	1.03	0.85	0.53	0.66		
	Ball shear %	100%	100%	100%	100%	100%		
	Ball lift %	0%	0%	0%	0%	0%		
Cu Wire/Al Pad	Min	22.98	30.86	30.849	31.569	21.933	21.027	20.385
	Avg	24.29	36.40	36.78	35.76	34.05	27.07	23.65
	Max	25.92	39.43	41.10	39.98	38.62	33.24	31.58
	Stdev	0.88	2.22	1.99	2.36	4.47	3.56	3.25
	Ball shear %	100%	100%	100%	100%	100%	100%	100%
	Ball lift %	0%	0%	0%	0%	0%	0%	0%
Cu Wire/Ni/Pd/Au Pad	Min	23.86	28.46	28.699	28.612	21.845	21.21	24.461
	Avg	30.42	34.82	33.18	32.74	30.27	28.64	28.19
	Max	36.42	41.36	38.39	37.00	34.01	34.55	32.66
	Stdev	2.95	2.21	2.39	2.21	2.16	3.07	2.16
	Ball shear %	100%	100%	100%	100%	100%	100%	100%
	Ball lift %	0%	0%	0%	0%	0%	0%	0%

was observed. However, Al deformation was not observed with 2.3 µm or 3.3 µm Ni/Pd/Au pads. The wire bond process window for Cu wire on an Ni/Pd/Au pad was wider than that of Cu wire on an Al pad. Thorough Cu wire bonding process optimization on Al pad to ensure minimal Al splashing and to maintain a certain Al remnant underneath the Cu ball was less of a concern in Cu bonding on an Ni/Pd/Au pad. The pad cratering test revealed no damage to the underlying BOA structures in both Au and Cu wires on an Al pad and an Ni/Pd/Au pad.

Table I summarizes the ball shear results after wire bonded strip thermal aging at 225°C for four splits of the study, Au and Cu wires on an Al pad and an 1.3 µm Ni/Pd/Au pad. Similar ball shear and wire pull results were observed for all three Ni/Pd/Au thicknesses, and therefore are not presented here. The table lists the ball shear statistics as well as the ball shear failure mode distribution. Figs. 14 and 15 graph the ball shear and ball shear per area (gf/mil^2) results. The Cu wire splits were taken to a much greater thermal aging duration, to 2016 h instead of 1008 h, in order to gain more insight into the welding interconnect quality of Cu wire.

The Au-Al intermetallics behavior observed in the study matched with findings from many thorough studies in previous publications. The ball shear strength of the Au-Al system increased significantly from time zero to 96 and 192 h, then dropped back down to the time zero level at 500 and 1000 h of 225°C baking. Figs. 16a, 16b, and 16c display the progression of the Au-Al ball shear failure mode. At time zero, the Au-Al system is sheared through a very thin intermetallic layer, thus shearing through the Al and leaving about 25% gold area on the bond pad. With thermal treatment, Au-Al intermetallics become

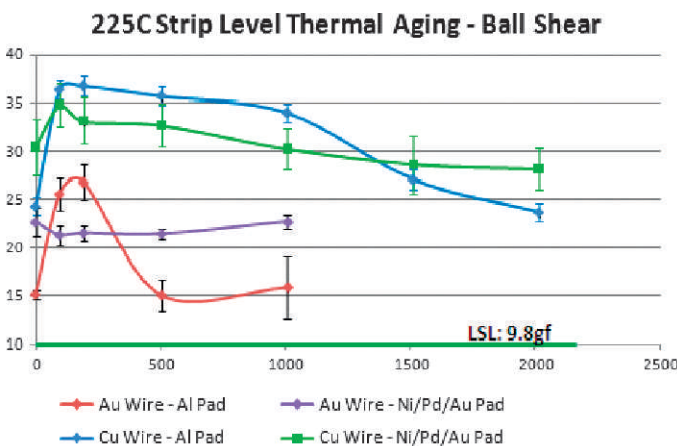

Fig. 14. Ball shear strength (gf) after 225°C strip-level thermal aging.

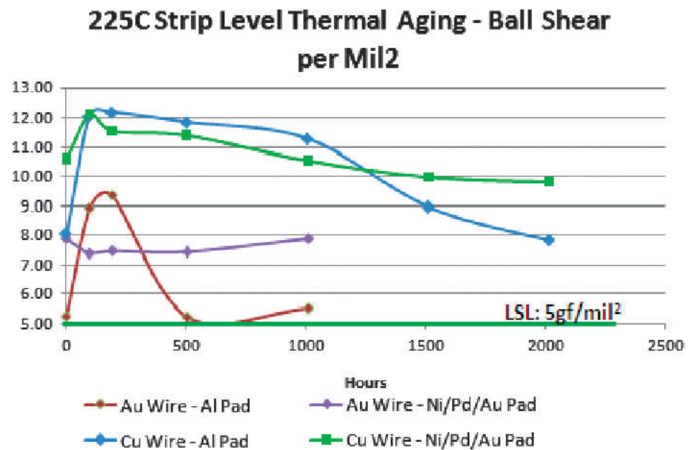

Fig. 15. Ball shear strength per area (gf/mil^2) after 225°C strip-level thermal aging.

Downloaded from http://meridian.allenpress.com/jmep/article-pdf/9/2/65/2248335/imaps_325.pdf by guest on 01 November 2022

(a) Au Wire / Al Pad at 0 Hour – Ball Shear with < 25% Au Remained

(b) Au Wire / Al Pad at 1008 Hours – Ball Shear with > 25% Au Remained

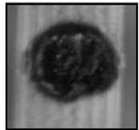

(c) Au Wire / Al Pad at 1008 Hours – Ball Shear with IMC Remained

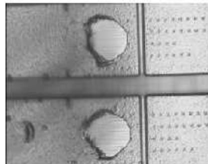

(d) Au Wire / OPM Pad at 0 Hour – Ball Shear

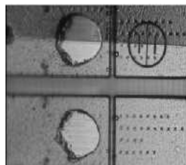

(e) Au Wire / OPM Pad at 1008 Hours – Ball Shear

Fig. 16. Ball shear failure mode for Au wire/Al Pad and Au wire/OPM pad.

thicker and stronger. Consequently, the shear tool shears through the bulk of the ball, leaving a thin disk of Au on the pad. With extended thermal baking, the Au-Al intermetallics start to degrade and the ball shearing test would shear through the interface between the intermetallics and the Au ball bond, thus leaving the intermetallics on the pad. The less desirable failure mode of the ball shear with intermetallics remaining on the pad also corresponds to lower ball shear strength at extended thermal duration.

The as-bonded ball shear strength of an Au wire on an Ni/Pd/Au pad is 50% higher than that of an Au wire on an Al pad. With the ball bond diameter measured nominally at 43 μm, the ball shear per area is calculated to be 7.9 gf/mil^2 and 5.3 gf/mil^2 for Au wire on Ni/Pd/Au and Al pads, respectively. In the Au wire / Ni/Pd/Au pad system, the ball shear strength stays constant at 22 gf (or 7.9 gf/mil^2) from time zero to 1000 h of 225°C thermal aging. Ball shear through the Au ball bond failure mode was observed in all thermal durations, as illustrated in Figs. 16d and 16e. This indicates that the Au-Au welding is extremely stable and stronger than the Au ball.

The as-bonded ball shear strength is 25% higher with Cu bonding on Ni/Pd/Au than on Al pads. The ball bond diameter was measured at nominal 44.1 μm and 43 μm for Cu wire on an Al pad and Cu wire on an Ni/Pd/Au pad, respectively. This

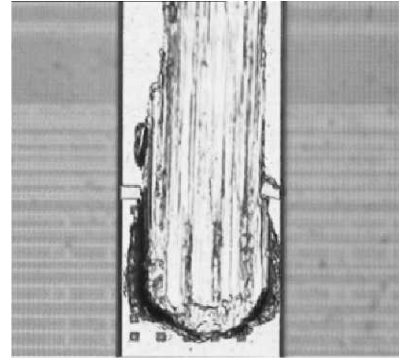

(a) Cu Wire / Al Pad at T0 – Al Smearing

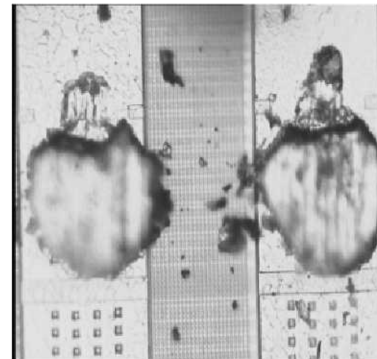

(b) Cu Wire / Al Pad at 2016hr Aging – Cu Bond Shear

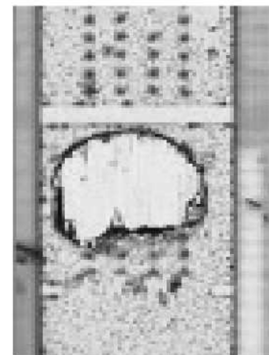

(c) Cu Wire / OPM Pad at T0 – Cu Bond Shear

(d) Cu Wire / OPM Pad at 2016hr Aging – Cu Bond Shear

Fig. 17. Ball shear failure mode for Cu wire/Al pad and Cu wire/OPM pad.

Downloaded from http://meridian.allenpress.com/jmep/article-pdf/9/2/65/2248335/imaps_325.pdf by guest on 01 November 2022

translates to a 2.5 gf/mil^2 (or more than 30%) improvement in ball shear per area for bonding on an Ni/Pd/Au pad (10.6 gf/mil^2) over bonding on an Al pad (8 gf/mil^2). At a high baking temperature of 225°C, the ball shear strength of the Cu ball on an Al pad increased significantly at 96 h, stayed relatively constant from 96 h to 1000 h, and then dropped back to the time-zero ball shear level at 1500 h. On the other hand, the ball shear strength of the Cu ball on an Ni/Pd/Au pad increased slightly at 96 h and decreased only slightly at longer aging duration.

Fig. 17 shows the difference in ball shear failure mode between Cu bonding on Al pad and Cu bonding on an Ni/Pd/Au pad. Although the ball shear failure mode was recorded for both systems, the specific shearing interface is completely different. In Fig. 17a for the Cu-Al system, the as-bonded shear failure mode occurs in the Al, indicated by Al smearing, since Al is substantially softer than Cu, and the Cu-Al intermetallics layer is extremely thin at time zero. As the thermal aging duration extended, the ball shear failure mode in the Cu wire/Al pad system evolved into shearing through the Cu ball bond, as shown in Fig. 17b. In the Cu wire/Ni/Pd/Au pad system with Ni being harder than Cu, the ball shear tool sheared through the Cu ball, leaving a thin layer of Cu on the pad. The same bond shear failure mode was recorded for Cu wire on an Ni/Pd/Au pad throughout the readpoints of the thermal aging study as shown in Figs. 17c and 17d. This indicates that the Cu ball is weaker than the Cu-Au or Cu-Pd bond. In fact, the ball shear test measures the strength of the Cu balls rather than the strength of the Cu-Au or Cu-Pd bond. The variation in the ball shear strength is most likely due to work hardening of the Cu balls.

Table II summarizes the wire pull strength and failure modes after 225°C strip-level thermal aging of Au and Cu wires on Al and Ni/Pd/Au pads. Fig. 18 graphs the wire pull integrity. As expected, pulling Au wire in the Au-Al system started out at breaking at the heat affected zone of the ball bond (i.e., the neck) and progressed to the ball lift failure mode at an extended duration of 1000 h of the high temperature bake at 225°C as the Au-Al intermetallics deteriorated. Consequently, the wire pull strength began with high strength with one failure mode of break-at-neck, then gradually decreased in strength with high variation at extended heat treatment due to the bimodal failure mode of break-at-neck and ball lift. By contrast, wire pull strength in Au wire/Ni/Pd/Au pad remained relatively constant throughout the heat treatment study with

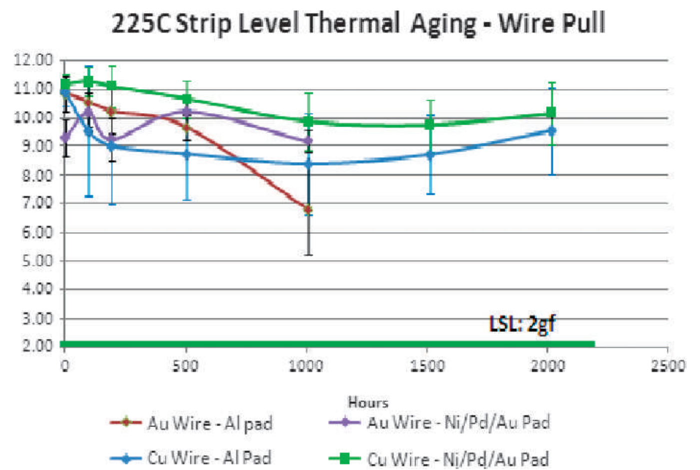

Fig. 18. Wire pull strength (gf) after 225°C strip-level thermal aging.

Table II
Wire Pull Strength (gf) After 225°C Strip-Level Thermal Aging

		0	96	192	504	1008	1512	2016
Au Wire/Al Pad	Min	8.945	9.395	9.168	8.95	3.62		
	Avg	10.87	10.56	10.24	9.68	6.81		
	Max	12.00	12.11	11.92	10.77	8.99		
	Stdev	0.63	0.88	0.74	0.42	1.61		
	Wire break %	100%	100%	100%	100%	47%		
	Ball lift %	0%	0%	0%	0%	53%		
	Pad peeling %	0%	0%	0%	0%	0%		
Au Wire/Ni/Pd/Au Pad	Min	7.79	9.177	8.1	9.39	8.44		
	Avg	9.30	10.21	9.26	10.22	9.19		
	Max	10.09	11.29	10.89	11.00	9.8		
	Stdev	0.65	0.69	0.77	0.54	0.40		
	Wire break %	100%	100%	100%	100%	100%		
	Ball lift %	0%	0%	0%	0%	0%		
	Pad peeling %	0%	0%	0%	0%	0%		
Cu Wire/Al Pad	Min	9.20	5.41	3.89	5.19	5.65	6.07	5.98
	Avg	10.88	9.55	9.03	8.74	8.41	8.72	9.56
	Max	11.61	11.83	11.93	11.07	11.09	10.75	11.86
	Stdev	0.49	2.27	2.07	1.58	1.79	1.38	1.51
	Wire break %	100%	50%	44%	44%	47%	53%	66%
	Ball lift %	0%	0%	0%	0%	0%	0%	0%
	Pad peeling %	0%	50%	56%	56%	53%	47%	34%
Cu Wire/Ni/Pd/Au Pad	Min	10.38	10.21	8.24	8.50	8.05	7.54	7.49
	Avg	11.18	11.28	11.11	10.67	9.88	9.76	10.17
	Max	11.81	12.07	11.94	11.75	11.75	11.19	11.91
	Stdev	0.39	0.51	0.74	0.66	0.99	0.92	1.09
	Wire break %	100%	100%	100%	100%	100%	100%	100%
	Ball lift %	0%	0%	0%	0%	0%	0%	0%
	Pad peeling %	0%	0%	0%	0%	0%	0%	0%

Downloaded from http://meridian.allenpress.com/imaps/article-pdf/9/2/65/2248335/imaps_325.pdf by guest on 01 November 2022

the same break-at-neck failure mode. Fig. 19 presents the two ball shear failure modes for Au wire.

The wire pull strength of Cu wire was higher than that of Au wire. For 23 μm wire diameter, the wire pull strength of Cu wire was recorded at 11 gf, about 10% higher than that of Au wire. Since Cu wire does not have as distinct a heat affected zone (HAZ) as Au wire, Cu wire does not break at the neck area but will be broken at the location where the wire pull tool (i.e., hook) is placed during the wire pull test. Fig. 20a presents a Cu wire that broke at the first kink where the wire pull hook was placed. The average wire pull strength of Cu wire on Al pad dropped after 96 h of thermal aging due to the change in failure mode from break at hook location to pad peeling. One example of pad peeling is shown in Fig. 20b. The wire pull strength of a pad peeling was recorded to be as low as 4 gf.

The micrograph in Fig. 20a contains two wires that were not pulled and two wires that were pulled. The unpulled wires have the original loop trajectory defined during wire bonding. The angle formed between the wire above the ball and the die surface is almost 90°. However, the loop trajectory is no longer present in the pulled wires. Since Cu wire has higher elongation than Au wire, it is much easier for the wire pull hook to stretch the wire and slip along the wire. As such, the angle between the wire and die surface is now less than 90°. The wire pull force generates more shear force against the ball bond. At high temperature baking, it is expected that the Cu wire would be further annealed and its microstructure would get larger. The softening Cu wire would cause further wire stretching during the wire pull test and higher shear force is applied onto the bond pad. Since Cu-low *k* silicon is used, the interlayer adhesion strength is lower than in earlier IC technology nodes [4]. When the shear force is larger than the ILD interlayer adhesion strength under the ball bond area, ILD delamination failure or pad peeling can occur with wire pull

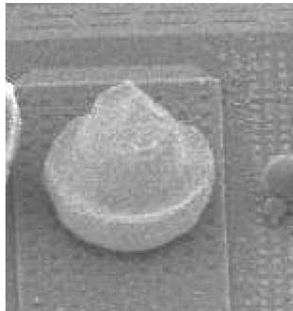

(a) Au Wire / Al Pad and Au Wire / OPM Pad – Break at Neck

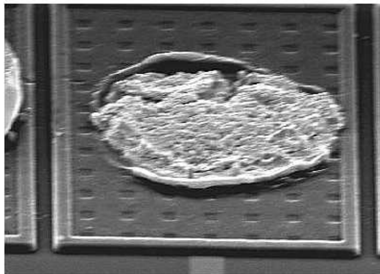

(b) Au Wire / Al Pad at 1008 Hours – Break at Au-Al IMC (Ball Lift)

Fig. 19. Wire pull failure mode for Au wire/Al pad and Au wire/Ni/Pd/Au pad.

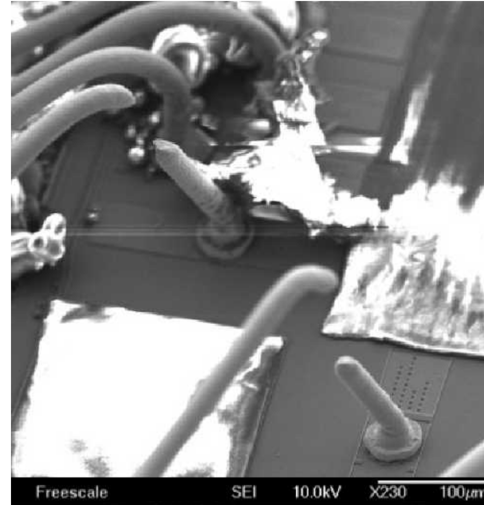

(a) Cu Wire / Al Pad and Cu Wire / OPM Pad – Break at Hook

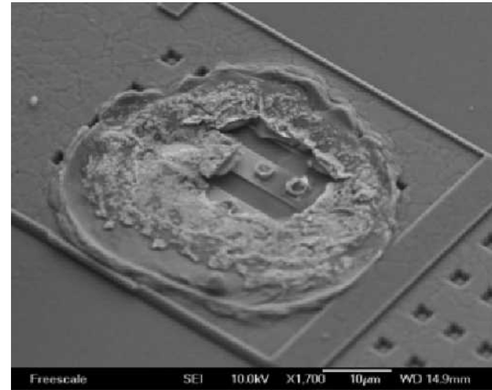

(b) Cu Wire / Al Pad at 96 Hour Bake 225C – Pad Peel

Fig. 20. Wire pull failure mode for Cu wire/Al pad and Cu wire/OPM pad.

testing [5, 6]. Although the wire pull failure mode switched to pad peeling at 96 h of thermal aging, the wire pull strength still far exceeds the minimum pull requirement, and thus is considered acceptable.

On the other hand, the wire pull strength of Cu wire on the Ni/Pd/Au pad essentially remained constant through the thermal treatment duration with the same failure mode of break at hook location. The result also indicates that the adhesion strength of the Ni/Pd/Au remetallization to the Al pad is higher than Cu wire strength. No pad peeling or OPM peeling was observed.

D. Package Reliability Results of Au and Cu Wires on Al and OPM Pads

Table III summarizes the electrical test results for Au and Cu wires on Al pad and three Ni/Pd/Au pad thicknesses packaged in 176 lead 24 × 24 mm LQFP after package reliability stresses. All eight splits passed 3000 air-to-air temperature cycling cycles (−65°C /150°C), and 2160 h of high temperature bake at 175°C. All splits except the two splits with 2.3 μm Ni/Pd/Au pads also passed 240 h of UHAST.

Eight packages from wafers plated with 2.3 μm Ni/Pd/Au had open circuit failures after 96 or 192 h of UHAST. Several

Downloaded from http://meridian.allenpress.com/jmep/article-pdf/9/2/65/2248335/imaps_325.pdf by guest on 01 November 2022

Table III
Package Reliability Electrical Test Results

Wire Type	Cell	MSL3/260°C + AATC-C (−65C to 150C)	MSL3/260C + UHAST (130°C/85% RH/33.3 PSIA)	HTB, 175°C
Au Wire	Al Pad	Passed 3000 cycles SS: 150	Passed 240 h SS: 150	Passed 2160 h SS: 150
	1.3 μm OPM	Passed 3000 cycles SS: 137	Passed 240 h SS: 137	Passed 2160 h SS: 137
	2.3 μm OPM	Passed 3000 cycles SS: 130	Failed 96 and 192 h Passed 240 h SS: 122	Passed 2160 h SS: 122
	3.3 μm OPM	Passed 3000 cycles SS: 125	Passed 240 h SS: 120	Passed 2160 h SS: 126
Cu Wire	Al Pad	Passed 3000 cycles SS: 115	Passed 240 h SS: 115	Passed 2160 h SS: 115
	1.3 μm OPM	Passed 3000 cycles SS: 72	Passed 240 h SS: 67	Passed 2160 h SS: 63
	2.3 μm OPM	Passed 3000 cycles SS: 150	Failed 96 h Passed 192 and 240 h SS: 149	Passed 2160 h SS: 148
	3.3 μm OPM	Passed 3000 cycles SS: 135	Passed 240 h SS: 134	Passed 2160 h SS: 134

packages were submitted to failure analysis. Upon removing the mold compound of the packages, ball lift was found at the failed signal pins. Fig. 21 presents one top-down optical example of a bond pad having Au ball lift. In Fig. 22a, the FIB micrograph of another open circuit failure ball shows a complete separation between the ball bond and the surface of Ni/Pd/Au pad. In Fig. 22c, the higher magnification photograph of the region outside the ball bond revealed unusually thick and thorny gold. The thorny Au surface was flattened during the wire bonding process as shown in Fig. 22b. These FIB cross sections clearly show similar thicknesses between Au and Pd layers, which is not normal for an Au immersion process. The comparison of the Au thickness from 3 Ni/Pd/Au thickness samples is presented in Fig. 23. While the Au thickness in 1.3 μm and 3.3 μm Ni/Pd/Au samples was close to the Au thickness specification of 50 nm, the Au thickness in 2.3 μm OPM samples was measured at 140 nm nominally and could be as thick as 220 nm.

The various regions underneath the Au ball bond were analyzed by EDX. The elemental composition of all regions except the Pd layer was as expected. The Pd layer revealed Ni trace similar to Fig. 8. The UHAST failure was due to poor bondability on a defective Au surface on the 2.3 μm Ni/Pd/Au splits, rather than an intrinsic failure.

Package samples from time zero, 2000 temperature cycling cycles, 96-h UHAST and 1080-h high temperature bake at 175°C were chemically deprocessed and wire pull and ball shear tests were performed to demonstrate capability of meeting AEC grade 0. Post stress ball shear data for Au and Cu wires on Al and 3 Ni/Pd/Au pads is summarized in Table IV. Ball shear of all eight splits was well above the minimum specification limit of 9.8 gf for 43 μm ball bond diameter, which is extrapolated from JEDEC JESD22-B116 standard.

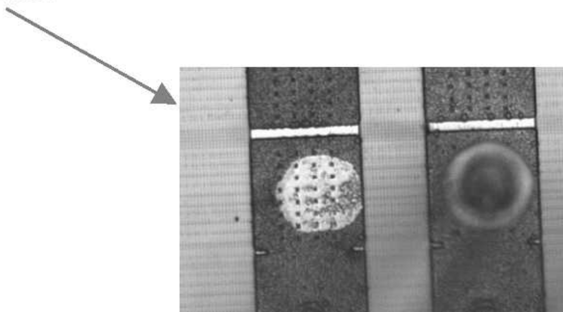

Fig. 21. Ball lift after 96-h UHAST on 2.3 μm Ni/Pd/Au pad.

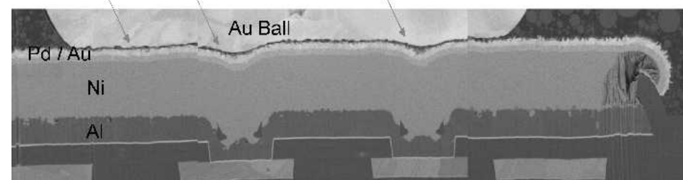

(a) Ball Bond Separating from Pad

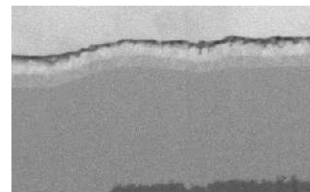

(b) Region Underneath Ball Bond

(c) Region Outside Ball Bond with Thorny Au

Fig. 22. Ball lift after 96-h UHAST on 2.3 μm Ni/Pd/Au pad.

Downloaded from http://meridian.allenpress.com/jmep/article-pdf/9/2/65/2248335/imaps_325.pdf by guest on 01 November 2022

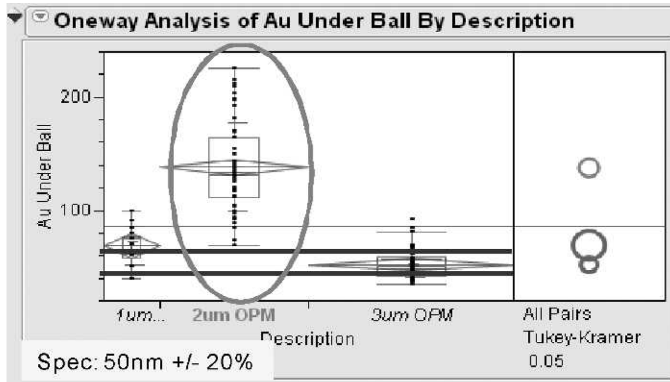

Fig. 23. Au thickness measurement from three Ni/Pd/Au thickness samples.

Table V summarizes the post stress wire pull data for the eight splits. A ball lift failure mode similar to Fig. 19(b) was found on the Au-Al split after temperature cycling and UHAST test. Although the minimum wire pull strength in the Au-Al split is much higher than the minimum specification limit of 2 gf, ball lift is not an acceptable failure mode for some automotive customers. A wire pull strength of Au wire on 1.3 µm and 3.3 µm Ni/Pd/Au pads remained relatively constant across the stress readpoints with 100% break-at-neck failure mode. Some ball lift failures similar to Fig. 21 occurred in the split of Au wire on the 2.3 µm Ni/Pd/Au pad and were attributed to the same root cause of thorny Au and resulting poor bonding quality. Wire pull results from the four Cu wire splits in general are very good, easily passing the minimum specification

Table IV
Post Stress Ball Shear Summary

(a) Ball shear for Au wire

Cell	Stats	T_0	MSL3/260°C + AATC-C (−65°C to 150°C) 2000 cycles	MSL3/260°C + UHAST (130°C/85% RH/33.3 PSIA)	HTB, 175°C 1080 h
Al Pad	Min	19.37	17.19	19.42	17.41
	Average	21.35	21.55	22.66	21.65
	Max	23.34	25.99	25.25	24.77
	Ball shear %	100%	100%	100%	100%
	Ball lift %	0%	0%	0%	0%
1.3 µm OPM	Min	19.10	18.39	21.02	18.47
	Average	21.16	23.62	22.75	22.99
	Max	23.25	25.63	24.87	25.07
	Ball shear %	100%	100%	100%	100%
	Ball lift %	0%	0%	0%	0%
2.3 µm OPM	Min	18.99	18.84	19.62	16.94
	Average	20.47	22.70	21.03	21.86
	Max	23.28	25.63	22.89	25.16
	Ball shear %	100%	100%	100%	100%
	Ball lift %	0%	0%	0%	0%
3.3 µm OPM	Min	19.09	20.11	21.23	18.34
	Average	20.95	24.07	22.50	21.46
	Max	22.54	25.72	23.84	25.45
	Ball shear %	100%	100%	100%	100%
	Ball lift %	0%	0%	0%	0%

(b) Ball shear for Cu wire

Cell	Stats	T_0	MSL3/260°C + AATC-C (−65°C to 150°C) 2000 cyc	MSL3/260°C + UHAST (130°C/85% RH/ 3.3 PSIA) 96 h	HTB, 175°C 1080 h
Al Pad	Min	20.87	16.99	19.91	20.91
	Average	23.12	19.41	22.71	27.61
	Max	24.84	22.08	25.53	33.19
	Ball shear %	100%	100%	100%	100%
	Ball lift %	0%	0%	0%	0%
1.3 µm OPM	Min	26.58	27.82	29.27	30.94
	Average	33.49	30.06	32.67	34.29
	Max	37.16	33.32	35.05	37.06
	Ball shear %	100%	100%	100%	100%
	Ball lift %	0%	0%	0%	0%
2.3 µm OPM	Min	27.51	28.14	25.48	14.34
	Average	29.50	31.14	32.60	26.74
	Max	34.38	34.11	36.95	36.40
	Ball shear %	100%	100%	100%	100%
	Ball lift %	0%	0%	0%	0%
3.3 µm OPM	Min	26.76	26.90	28.37	19.13
	Average	30.32	31.16	32.11	29.69
	Max	34.31	38.84	35.55	40.26
	Ball shear %	100%	100%	100%	100%
	Ball lift %	0%	0%	0%	0%

Downloaded from http://meridian.allenpress.com/jmep/article-pdf/9/2/65/2248335/imaps_325.pdf by guest on 01 November 2022

Table V
Post Stress Wire Pull Summary

(a) Wire pull for Au wire

Cell	Stats	T_0	MSL3/260°C + AATC-C (-65°C to 150°C) 2000 cyc	MSL3/260°C + UHAST (130°C / 85% RH / 33.3 PSIA)	HTB - 175°C 1080 h
Al Pad	Min	7.63	4.09	6.05	6.45
	Average	8.39	8.14	7.84	8.62
	Max	8.95	9.14	8.49	9.90
	Wire break %	100%	84%	94%	0%
	Ball lift %	0%	16%	6%	0%
	Pad peel %	0%	0%	0%	0%
1.3 µm OPM	Min	7.85	8.26	7.31	3.21
	Average	8.92	8.84	8.39	9.08
	Max	9.86	9.69	9.36	9.74
	Wire break %	100%	100%	100%	100%
	Ball lift %	0%	0%	0%	0%
	Pad peel %	0%	0%	0%	0%
2.3 µm OPM	Min	2.45	3.94	6.14	3.94
	Average	8.03	8.29	8.29	8.51
	Max	9.31	9.10	9.26	9.49
	Wire break %	91%	91%	100%	97%
	Ball lift %	9%	9%	0%	3%
	Pad peel %	0%	0%	0%	0%
3.3 µm OPM	Min	8.31	7.60	7.43	7.91
	Average	8.86	8.88	8.59	8.79
	Max	9.68	9.75	9.29	9.69
	Wire break %	100%	100%	100%	100%
	Ball lift %	0%	0%	0%	0%
	Pad peel %	0%	0%	0%	0%

(b) Wire pull for Cu wire

Cell	Stats	T_0	MSL3/260°C + AATC-C (−65°C to 150°C) 2000 cycles	MSL3/260C + UHAST (130°C/85% RH/33.3 PSIA) 96 h	HTB - 175°C 1080 h
Al Pad	Min	9.12	8.33	8.83	5.44
	Average	9.99	9.94	10.03	9.54
	Max	10.76	11.06	13.45	10.88
	Wire break %	100%	100%	100%	94%
	Ball lift %	0%	0%	0%	0%
	Pad peel %	0%	0%	0%	6%
1.3 µm OPM	Min	8.94	7.09	8.49	8.05
	Average	9.82	8.46	9.75	9.25
	Max	10.67	9.54	10.59	10.39
	Wire break %	100%	100%	100%	100%
	Ball lift %	0%	0%	0%	0%
	Pad peel %	0%	0%	0%	0%
2.3 µm OPM	Min	7.83	5.54	8.19	5.06
	Average	8.65	8.92	9.77	9.54
	Max	9.31	10.19	10.70	11.06
	Wire break %	100%	100%	100%	92%
	Ball lift %	0%	0%	0%	8%
	Pad peel %	0%	0%	0%	0
3.3 µm OPM	Min	7.76	4.84	4.20	8.02
	Average	8.82	8.97	8.74	8.98
	Max	9.86	9.99	10.14	9.71
	Wire break %	100%	100%	98%	100%
	Ball lift %	0%	0%	2%	0%
	Pad peel %	0%	0%	0	0%

limit of 2 gf. A few pad peel failure modes, as shown in Fig. 20b, were recorded in the Cu-Al split at 1080 h of high temperature bake, still with a minimum reading of over 5 gf. Some ball lift failures due to thorny Au were also found on 2.3 µm and 3.3 µm Ni/Pd/Au pads with Cu wires. This data suggests wafer-to-wafer variation in the plating quality that requires further process improvement.

Sample packages after 1080 h of high temperature bake at 175°C were submitted to cross sectioning for ball bond and interface integrity inspection. Fig. 24 presents examples of cross sections of Au and Cu wires on Al and 1.3 µm Ni/Pd/Au pads. In Fig. 24a, as expected in the Au wire/Al pad system, the Al pad was fully consumed, and thick Au-Al intermetallics and large Kirkendall voiding were found. On the other hand, in

Downloaded from http://meridian.allenpress.com/jmep/article-pdf/9/2/65/2248335/imaps_325.pdf by guest on 01 November 2022

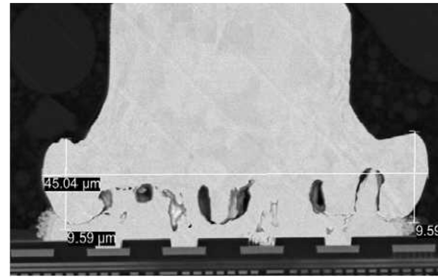

(a) Au Wire on Al Pad

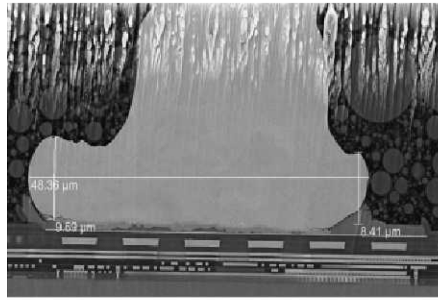

(b) Cu Wire on Al Pad

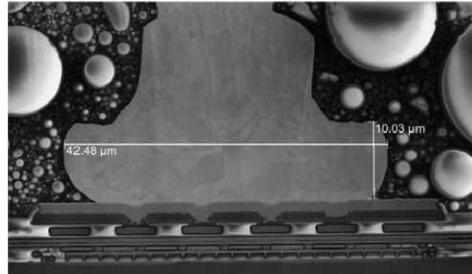

(c) Au Wire on OPM Pad

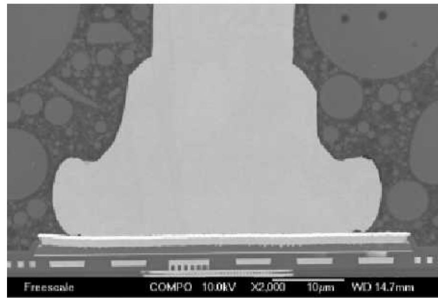

(d) Cu Wire on OPM Pad

Fig. 24. Cross sections of ball bonds after 1080 h of high temperature bake at 175°C.

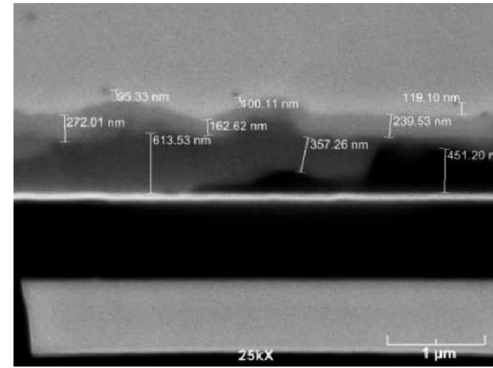

(a) Cu Ball on Al Pad

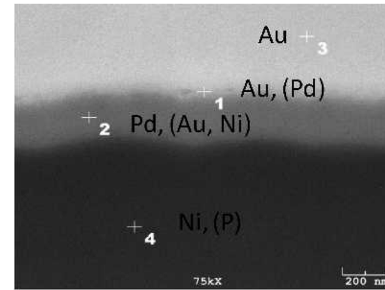

(b) Au Ball on OPM Pad

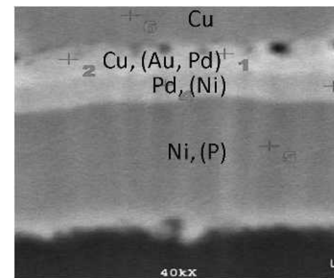

(c) Cu Ball on OPM Pad

Fig. 25. High magnification of interface region after 1080 h of high temperature bake at 175°C.

the Cu wire/Al pad system, the aluminum was not fully consumed into the intermetallics. The combined intermetallic region was only about 0.9 μm thick. No Kirkendall voiding was observed along the interface. Fig. 25a presents a higher magnification of the Cu-Al intermetallic region. EDX revealed the intermetallic region closer to the Cu ball to be Cu_9Al_4 and the intermetallic region closer to the Al pad to be a mixture of CuAl and $CuAl_2$, which is in agreement with previous publications [5-8].

The interface between Au wire and Cu wire on an Ni/Pd/Au pad remained relatively unchanged from time zero to 1080 h of high temperature bake. Higher magnification micrographs at the center of the Au and Cu ball bonds on Ni/Pd/Au pad after 1080 h of high temperature bake at 175°C are shown in Figs. 25b and 25c, respectively. No intermetallics formation was observed for Au wire or Cu wire on an Ni/Pd/Au pad. The strong bond strength is presumably related to the full intersolubility of the metals along these interfaces [9-12]. Ni trace in the Pd layer was due to the defective Pd process and will be corrected in the next evaluations.

Cu wire bonding on an Al pad and an Ni/Pd/Au pad, and Au wire bonding on an Ni/Pd/Au pad, are equally reliable within the testing durations evaluated in this study. Ball shear and wire pull strengths of these three systems are well above the minimum specification limits, and the failure modes satisfy specific automotive customers. The three systems met and exceeded package-level reliability stress tests specified for AEC grade 0. Ni/Pd/Au pad offers specific advantages over Al pad when using copper wire. Ni/Pd/Au pad enables a wider wire bond process window. The need to minimize Al splashing and optimize the Al remnant underneath the ball bond is eliminated. The wire pull failure mode of pad peeling observed in Cu wire bonding on Al pad is also eliminated. This is critical

Downloaded from http://meridian.allenpress.com/jmep/article-pdf/9/2/65/2248335/imaps_325.pdf by guest on 01 November 2022

for some automotive customers who require good wire pull strength and accept only the wire break failure mode.

Conclusions and Recommendations

- Au and Cu wire bonding on low-*k*-copper wafers with the conventional aluminum pad and electroless nickel/electroless palladium/immersion gold OPM were studied for high temperature applications.
- Plating defects associated with Ni/Pd/Au (OPM) plating that can cause yield loss were evaluated. Two types of nonuniform plating, very uneven plating of nickel within a single pad and nonuniform, thorny, and thicker gold plating (more than five times the expected Au immersion thickness) were found to be defects that cause NSOP yield losses.
- When Au grows thicker than expected for an immersion process, it is inferred to be due to the defective Pd layer and subsequent Ni diffusion. The thorny appearance of Au leads to defective bonding and ball lifting.
- Nodular plating growth, especially along the periphery of the bond pad, was shown to lead to electrical short failure, especially when the bond pad separation is limited to 10 µm or less.
- As plating defects leading to NSOP cannot be detected by electrical testing at post OPM probing, it is recommended to establish a plating defect inspection system in order to detect these defects.
- Based on packaging reliability evaluations such as device reliability and capability to withstand bonding forces, it is recommended to have an OPM thickness of 1.8 µm for pad separation of 10 µm and passivation height of about 1 µm.
- Strip-level thermal aging at 225°C showed robust reliability for OPM surface for high temperature applications.
- For the Au wire/Ni/Pd/Au pad system, the ball shear strength remains constant from time zero to 1000 h of 225°C thermal aging. Ball shear through the Au ball bond failure mode was observed for all thermal durations, indicative of very stable Au-Au bonding which was stronger than the Au ball. On the other hand, Au on Al shows degradation with thermal aging due to IMC formation and Kirkendall voiding.
- The problem of Al splashing with Cu wire bonding on an Al pad was found to be completely eliminated by switching to Cu wire bonding on an Ni/Pd/Au pad.
- The wire pull strength of Cu wire on an Ni/Pd/Au pad remained constant through any thermal treatment duration with the same failure mode of break at hook location.
- The adhesion strength of the Ni/Pd/Au remetallization to the Al pad is found to be higher than the Cu wire strength. No pad peeling or OPM peeling was observed.
- No intermetallics formation was observed for Au wire or Cu wire on the Ni/Pd/Au pad.
- Au wire on OPM passed post stress electrical tests at AATC (−65/150°C) 3000 cycles, HTB 175°C for 2160 h and UHAST for 240 h. Au/OPM splits also passed wire pull and ball shear testing after thermal aging, demonstrating excellent thermal stability and reliability of Au wire on OPM structures.
- Cu wire on Al and OPM passed electrical tests at AATC (−65/150°C) 3000 cycles, HTB 175°C for 2160 h and UHAST for 240 h. Cu/Al and Cu/OPM splits also passed wire pull and ball shear testing after thermal aging, demonstrating excellent thermal stability and reliability of Cu wire on both Al and OPM structures.

Acknowledgments

The authors thank the following people for their support in their respective areas of expertise: K.Y. Yow and Wen Shi Koh from Kuala Lumpur Malaysia (KLM) for their dicing expertise; P.L. Eu, Y.K. Au and Tracy Yap from Kuala Lumpur Malaysia (KLM) for their wire bond process expertise; Mike Ascerno and Toan Trinh for providing package reliability stressing and electrical test support; Julie Nadeau-Heineke, Anne Anderson, Chuck Petri, Alvin Youngblood, and Roy Ardlt for performing package cross-sectioning, SEM, FIB, and EDX analyses; Diana Mitro and Mike Mangrum for package failure analyses; Les Postlethwait and Yvette Meche for package deprocessing and performing ball shear and wire pull tests.

References

[1] L. Xu, "*Reliability tests of Cu wire bonded integrated circuits*, MS Thesis, Texas Tech University, Lubbock, https://dspace.lib.ttu.edu/, 2009.

[2] N. Srikanth, J. Premkumar, M. Sivakumar, Y.M. Wong, and C.J. Vath, "Effect of wire purity on copper wire bonding," in Proceedings of the 9th Electronics Packaging Technology Conference, pp. 755-759, 2007.

[3] C. Lee, T. Tran, B. Williams, and J. Ross, "Novel method of separating probe and wire bond regions without increasing die size and reducing weak Fab-BEOL adhesion interfaces," Journal of Microelectronics and Electronic Packaging, Vol. 3, No. 1, pp. 1-11, 2006.

[4] C. Goldberg, S. Downey, V. Fiori, R. Fox, K. Hess, O. Hinsinger, A. Humbert, J.-P. Jacquemin, S. Lee, J.-B. Lhuillier, S. Orain, S. Pozder, L. Proenca, F. Quercia, E. Sabouret, T.A. Tran, and T. Uehling, "Integration of a mechanically reliable 65-nm node technology for various substrate, interconnect, and package types," in Proceedings of the IEEE 2005 International Interconnect Technology Conference, pp. 3-5, 2005.

[5] S. Lee and L.M. Higgins, "Challenges of Cu wire bonding on low K/Cu wafers with BOA structures," in Proceedings of the 60th Electronic Components and Technology Conference ECTC, pp. 342-349, 2010.

[6] T. Tran, C.-C. Lee, V. Matthew, and L.M. Higgins, "Copper wire bonding on low-k/copper wafers with bond over active (BOA) structures for automotive customers," in Proceedings of the 61st Electronic Components and Technology Conference, ECTC, pp. 1508-1515, 2011.

[7] F.W. Wulff, C.D. Breach, Saraswati, and D. Stephan, "Characterization of intermetallic growth in copper and gold ball bonds on aluminum metallization," in Proceedings of the 6th Electronics Packaging Technology Conference, EPTC, 2004.

[8] F.W. Wulff, C.D. Breach, Saraswati, K. Dittmer, and M. Garnier *et al*, "Further characterization of intermetallic growth in copper and gold ball bonds on aluminum metallisation," in Proceedings of SEMICON, 2005.

[9] B. Chylak, J. Ling, H. Clauberg, and T. Thieme, "Next generation nickel-based bond pads enable copper wire bonding," Electrochemical Society Transactions, Vol. 18, No. 1, pp. 777-785, 2009.

[10] H. Clauberg, P. Backus, and B. Chylak, "Nickel-palladium bond pads for copper wire bonding," Microelectronics Reliability Journal, Vol. 51, No. 1, pp. 75-80, 2011.

[11] P.L. Eu, Z.S. Poh, Y.K. Au, C.C. Yong, T.A. Tran, J. Arthur, H. Downey, V. Mather, and Y.Y. Chee, "High temperature automotive application: A study on fine pitch Au and Cu WB integrity vs. Ni thickness of Ni/Pd/Au bond pad on C90 low-k wafer technology," in Proceedings of the 12th Electronics Packaging Technology Conference EPTC, pp. 349-354, 2010.

[12] P. Ratchev S. Stoukatch, and B. Swinnen, "Mechanical reliability of Au and Cu wire bonds to Al, Ni/Au and Ni/Pd/Au capped Cu bond pads," Microelectronics Reliability Journal, Vol. 46, No. 8, pp. 1315-1325, 2006.

Downloaded from http://meridian.allenpress.com/jmep/article-pdf/9/2/65/2248335/imaps_325.pdf by guest on 01 November 2022